Int. J. Electrochem. Sci., 14 **(2019)** 3393 – 3407, doi: 10.20964/2019.04.19

International Journal of ELECTROCHEMICAL SCIENCE
www.electrochemsci.org

Development of a Boron-Doped Diamond Electrode for the Simultaneous Detection of Cd^{2+} and Pb^{2+} in Water

JingXuan Pei[1], *Xiang Yu*[1,*], *Chao Zhang*[2] *and XingJu Liu*[3]

[1] Beijing Key Laboratory of Materials Utilisation of Nonmetallic Minerals and Solid Wastes, National Laboratory of Mineral Materials, School of Materials Science and Technology, China University of Geosciences (Beijing), 29 Xueyuan Road, Haidian, Beijing 100083, China
[2] School of Mechanical Engineering, Tianjin College, University of Science and Technology Beijing, No.1, North Ring Road, Zhujiang, Beijing-Tianjin New City, Baodi District, Tianjin 100083, China
[3] School of Engineering and Technology, China University of Geosciences (Beijing), 29 Xueyuan Road, Haidian, Beijing 100083, China
[*]E-mail: yuxiang@cugb.edu.cn

Received: 4 December 2019 / *Accepted:* 10 January 2019 / *Published:* 10 March 2019

Mercury film electrodes used in in-situ monitoring systems suffer from the drawbacks of secondary pollution and attenuation. To overcome these problems, a boron-doped diamond (BDD) film electrode was developed that was non-polluting and could be used for simultaneous detection and long durations. The concentrations of Cd^{2+} and Pb^{2+} in mixed solution were measured simultaneously, and the detection performances of the mercury film and BDD electrodes were systemically compared, to evaluate the feasibility of replacing mercury film electrodes with BDD electrodes. The effects of enrichment time and electrode surface state on the stripping peak currents of Cd^{2+} and Pb^{2+} were investigated. Optimum conditions were an enrichment time of 200 s and a hydrogen terminated electrode surface state. The optimized BDD electrode exhibited good performance characteristics: 1) The linear relationship between the ion concentration and the peak current was excellent (linear correlation coefficients (R^2) of the calibration curves for Cd^{2+} and Pb^{2+} were 0.995 and 0.998, respectively). The spiked recovery ranges of Cd^{2+} and Pb^{2+} in three spike experiments were 93.5% to 99.4% and 93.7% to 101.3%, respectively. 2) The detection limits for Cd^{2+} and Pb^{2+} were low, 3.39 μg/L and 3.62 μg/L, respectively. The BDD electrode had good reproducibility: relative standard deviations (RSD) of Cd^{2+} and Pb^{2+} obtained from 7 replicate experiments were 1.603% and 3.819%, respectively. After comprehensive data comparison of the detection performance for mercury film and BBD electrodes, it was concluded that the BDD electrode could replace mercury film electrodes in in-situ monitoring systems, having the advantage of allowing simultaneous detection, being non-polluting, and able to function for long-durations.

Keywords: Boron-Doped Diamond Film; Mercury Film Electrode; Heavy Metal Ions; Square Wave Anodic Stripping Voltammetry

1. INTRODUCTION

In-situ monitoring of heavy metal ions is the only way to prevent pollution of water sources in rural areas. Unfortunately, the mercury film electrodes used in current in-situ monitoring systems cannot meet the long duration operating requirements for the non-polluting, simultaneous detection of heavy metal ions. A typical example is heavy metal pollution in water sources in rural areas of Hubei Province, China. Researchers at China University of Geosciences (Wuhan) used the Chinese National Standards for Drinking Water Quality (GB 5749-2006) as a reference to investigate the status of heavy metal ion pollution in water sources in rural areas of Hubei Province [1]. The highest concentration of Cd^{2+} (335.58 μg/L) was in Huangshi and was 67 times higher than the permitted level. In Yichang, the highest concentration of Pb^{2+} was 177.50 μg/L, which was 17.7 times higher than the permitted level. Pollution of water sources has affected 94.9% of water in Jianli County, causing a prevalence of trematodiasis and water-borne diseases. In-situ monitoring of the concentrations of heavy metal ions in water sources is the only way to prevent pollution. However, rural areas are remote, have poor detection conditions, and cannot be manually monitored in real time. In addition, water sources affect downstream waters, so it is essential that the detection process does not damage the environment and is pollution-free. Testing conditions in rural areas and testing requirements for water sources require that the detection electrodes used in the in-situ monitoring system are capable of simultaneous detection, able to operate for long durations, and are non-polluting. Due to its high sensitivity and fast detection speed, square wave anodic stripping voltammetry has been the first choice for in-situ monitoring systems [2]. However, the most commonly used electrode, the mercury film electrode, cannot meet the proposed operating requirements, as the mercury in the electrode may cause secondary pollution of the water body. As the number of detections increases, heavy metal ions accumulate on the surface of the mercury film electrode and the detection performance of the electrode deteriorates [3-5]. The characteristics of boron-doped diamond (BDD) electrodes (non-polluting, good stability, and wide electrochemical window) can overcome many of the disadvantages of the mercury film electrode for the simultaneous detection of Cd^{2+} and Pb^{2+} [6]. Ti (titanium) interlayer is a good candidate for BDD preparation due to its high electrical conductivity and favorable film-substrate adhesion with the diamond film [7]. Therefore, the development of BDD electrodes that can detect Cd^{2+} and Pb^{2+} simultaneously, without causing pollution, and that meet the requirements for long duration operation, would be the key to improving in-situ water quality monitoring systems.

The application of the BDD electrodes in the field of water quality detection has so far focused on organic matter and single heavy metal ions. There is a lack of systematic research on the simultaneous detection of two heavy metal ions [8-10]. Direct comparison of the mercury film electrode and the BDD electrode are hindered by the lack of information on operating parameters and detection performance for BDD electrodes, in particular: 1) *The influence of the enrichment time and electrode surface state on the stripping peak currents of Cd^{2+} and Pb^{2+}*. The enrichment time affects the number of ions stripped on the surface of the electrode; the surface state affects the reaction processes of the ions. 2) *The calibration curve and spike recovery of the BDD electrode for simultaneous detection of Cd^{2+} and Pb^{2+}*. The calibration curve determines the detection precision of the electrode; the spike recovery reflects the accuracy of the electrode. Good detection precision and

accuracy are the crucial for BDD electrodes if they are to achieve their potential in environmental monitoring. 3) *The detection limits and reproducibility of the BDD electrode for the detection of Cd^{2+} and Pb^{2+}*. The detection limit represents the detection capability of the electrode; the reproducibility represents the precision and regeneration of the electrode. The low detection limits and good regeneration ability allow the BDD electrode to significantly improve on the performance of the mercury film electrode. Consequently, comprehensive investigations of the enrichment time and electrode surface conditions and their impact on the electrode detection performance are required. This will allow a thorough comparison of the detection performance of BDD electrodes and mercury film electrodes, to assess the feasibility of replacing the mercury film electrode with the BDD electrode.

In this study, a BDD electrode was prepared and used for the simultaneous detection of Cd^{2+} and Pb^{2+} in a mixed solution. The microstructure and electrochemical properties of the BDD electrode were characterized, and the effects of electrode enrichment time and surface state on the stripping peak current of Cd^{2+} and Pb^{2+} investigated. The operating parameters of the BDD electrode were optimized, and the detection performance of the BDD electrode and mercury film electrode was systematically compared.

2. EXPERIMENTAL

2.1 Equipment and reagents

BDD electrodes were prepared using an HF880 hot filament chemical vapor deposition apparatus (Langfang Siboer Diamond Technology Co., Ltd.). The electrode microstructure was characterized using an S-5500 scanning electron microscope (Hitachi, Ltd.). A CHI660E electrochemical workstation (Shanghai Chenhua Instrument Co., Ltd.) was used to measure the cyclic voltammetry curve of the electrode and to detect the heavy metal ions in a mixed solution. The working electrode was a BDD electrode and the reference electrode was a saturated calomel electrode (3 M KCl). A platinum electrode was used as the auxiliary electrode.

All compounds used were analytically pure. A standard solution of a mixture of $Cd(NO_3)_2$ and $Pb(NO_3)_2$ was prepared by adding deionized water to a 1000 mg/L atomic absorption standard prepared by the National Institute of Standards Materials. In the measurement of the cyclic voltammetry curve, 0.2 mol/L Na_2SO_4 solution was used as the supporting electrolyte. A NaAc-HAc buffer solution was used as the bottom liquid for the test. Sodium sulfate, sodium acetate and acetic acid were purchased from Shanghai Pharmaceuticals Holding Co., Ltd. The working electrode base material was a titanium plate, the boron source was B_2O_3, the carbon source in the nucleation stage was CH_4, the carbon source in the growth stage was C_2H_5OH, and the etching gas was H_2.

2.2 Preparation and characterization of the BDD electrode

Preparation of Ti/BDD electrodes. In the pretreatment stage, the substrate was first smoothed with sandpaper and polished to a mirror surface. The substrate was then ultrasonically cleaned in

acetone for 20 min and dried. Finally, the substrate was ultrasonically seeded in a 2.4% w/w suspension of nano-diamond powder in ethanol for 10 min, dried and placed in a reaction chamber. In the coating stage, a solution of B_2O_3 in C_2H_5OH was introduced into the reaction chamber with H_2. The C/H ratio was set to 2.4% and the B/C ratio was 6‰. Ta wires provided a heat source with a nucleation time of 0.5 h, and H_2:CH_4 of 1000:10 sccm. A growth time of 7.5 h, and H_2 (bubble):C_2H_5OH+H_2+B_2O_3:H_2 of 25:50:1000 sccm was used. The pressure was 3000 Pa and the deposition temperature was 700 °C.

Characterization of film formation quality and electrochemical performance of BDD electrodes. The overall morphology and average particle size of the surface of the electrode were analyzed to characterize the film formation quality of the diamond film. The surface element distribution of the electrode was analyzed with an energy dispersive spectrometer (EDS) to characterize the doping of boron. The cyclic voltammetry curve of the electrode was measured to analyze the potential window and background current of the electrode; the scanning range was -1.8 V to +1.4 V, the scanning speed was 50 mV/s, the initial potential was 0.003 V, and the step potential was 2 mV.

2.3 Simultaneous detection of Cd^{2+} and Pb^{2+} in a mixed solution

Preparing different types of electrode termination. A hydrogen-terminated and an oxygen-terminated BDD electrode were prepared by electrochemical polarization. The electrode was polarized using an electrochemical workstation. The oxygen-terminated BDD electrode was obtained with a voltage of +1.8 V and a polarization time of 120 s. The hydrogen-terminated BDD electrode was obtained with a voltage of -1.8 V and a polarization time of 120 s.

Simultaneous detection of Cd^{2+} and Pb^{2+} in a mixed solution. Square wave stripping voltammetry was used with a stripping frequency of 25 Hz, an amplitude of 20 mV, a step potential of 2 mV, a deposition potential of -0.8 V, and a scanning range of -0.8 V to +0.8 V. The standard mixture was composed of 0.01 mg/L of Cd^{2+} and 0.05 mg/L of Pb^{2+} with a pH of 4.68.

3. RESULTS AND DISCUSSION

3.1 Microstructure and cyclic voltammetry curve of the BDD electrode

3.1.1 Microstructure of the BDD electrode

Doping boron into the diamond film to form a P-type semiconductor can improve the electromigration capability of a thin film electrode. The microstructure of the electrode directly affects its electrochemical performance.

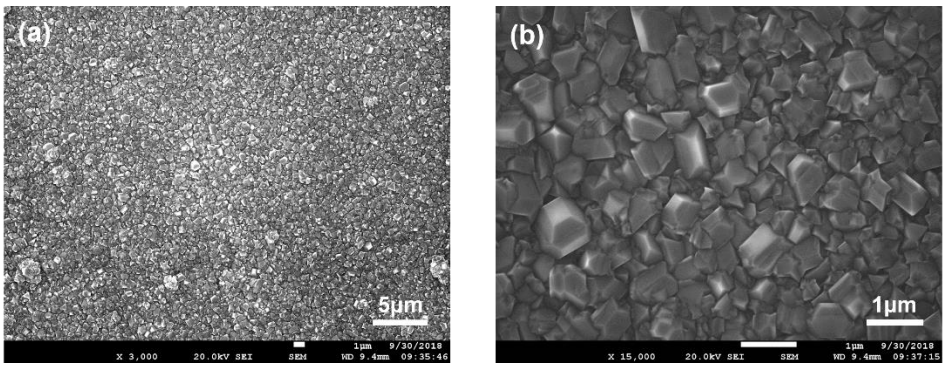

Figure 1. SEM images of a BDD electrode at different magnifications: (a) 3,000 times; (b) 15,000 times

As can be seen from Fig. 1(a), the crystal grains of the prepared BDD electrode grew fast and were closely packed to form a dense continuous film. Fig. 1(b) shows that the diamond crystals had a sharp angular shape and an average particle diameter of about 650 nm. Such nano-sized grains are beneficial for increasing the effective working area of the electrode but may cause an increase in the electrode background current [11].

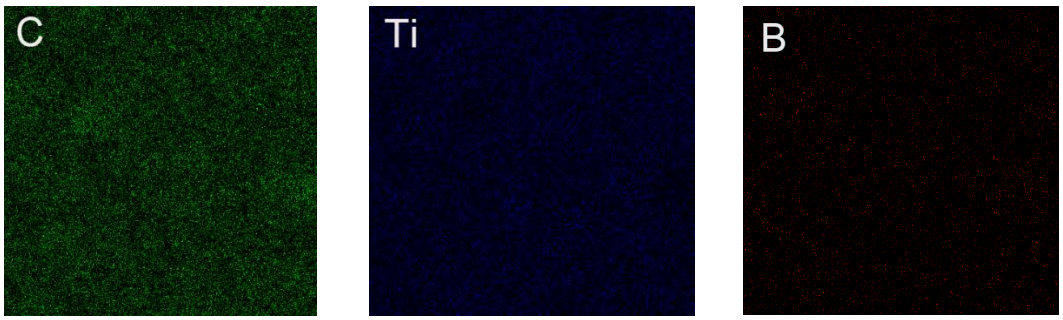

Figure 2. Distribution of three elements on the surface of BDD electrode

It can be seen from Fig. 2 that the surface of the BDD electrode was mainly distributed with three elements: carbon in the diamond film, titanium in the matrix material, and boron doped into the diamond film. The very small amount of boron was uniformly distributed on the surface of the electrode. This distribution indicates that the boron was successfully doped in the diamond film. The uniform distribution of boron on the electrode surface improves the stability of the detection performance.

3.1.2 Cyclic voltammetry curve of the BDD electrode

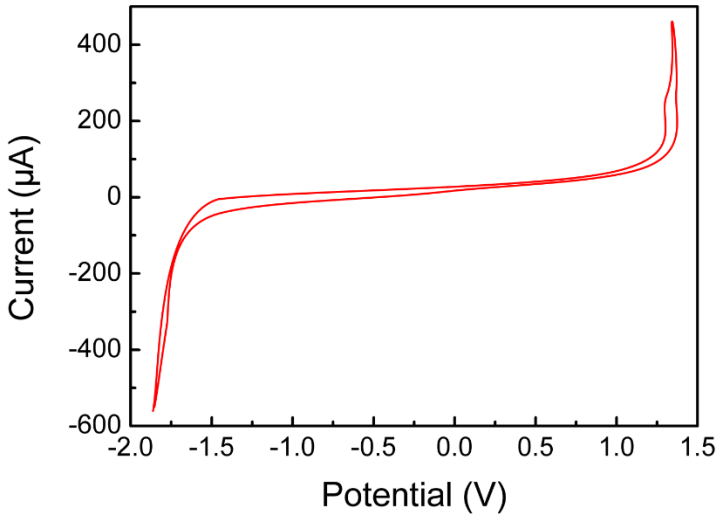

Figure 3. Cyclic voltammetry curve of a BDD electrode in a 0.2 M Na_2SO_4 solution. The number of cycles was 10 laps; the scanning speed was 50 mV/s; the step potential was 2 mV.

As can be seen from Fig. 3, the potential window of the BDD electrode was effective in the range of -1.5 V to +1.2 V (ΔU = 2.7 V). The potential window is determined by the hydrogen evolution and oxygen absorption reactions of the electrode, and the electron transfer in the reaction process is realized by the reaction intermediate adsorbed on the surface of the electrode. The B–C (sp^3) moiety on the surface of the BDD electrode has a weak adsorption capacity for the reaction intermediate, resulting in an extremely wide potential window of the electrode [12]. The potential window of 2.7 V for this electrode allows the simultaneous detection of Cd^{2+} and Pb^{2+}. The background current of the electrode had a fairly large range of -70 μA to 85 μA. The background current is affected by the electric double layer capacitance of the electrode surface. The growth orientation of the diamond grains was not uniform, resulting in the presence of a microelectrode distribution on the electrode surface. The separation of the active sites causes the electric double layer capacitance to decrease, which in turn causes the background current to decrease [13]. Excessive background current increases energy consumption and reduces current efficiency; it is also detrimental to de-spectral processing when detecting ions. These results indicated that a thin film electrode prepared using these process parameters had been successfully doped with boron. The electrode was well crystallized and had a wide potential window and a low background current, enabling simultaneous detection of Cd^{2+} and Pb^{2+}.

3.2 Effect of enrichment time and electrode surface state on stripping peak currents of Cd^{2+} and Pb^{2+}

3.2.1 Effect of enrichment time on stripping peak currents of Cd^{2+} and Pb^{2+}

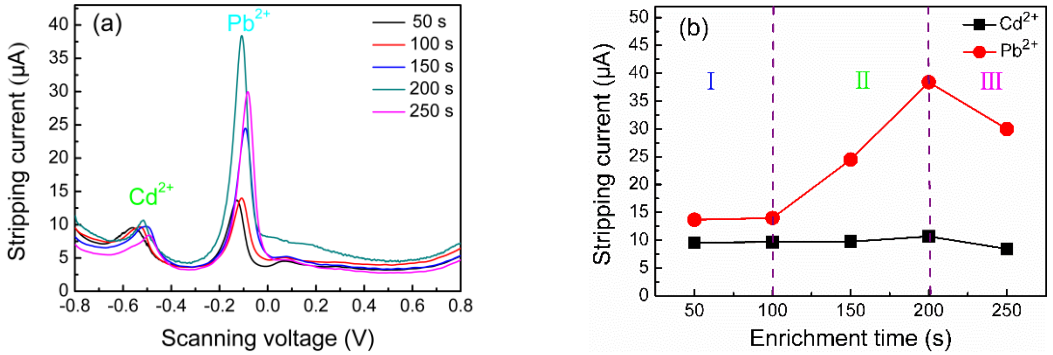

Figure 4. Curves of the stripping current intensity of Cd^{2+} and Pb^{2+} as a function of enrichment time: (a) Five enrichment times; (b) The two ions' stripping peak currents. The deposition potential was -0.8 V; the stripping frequency was 25 Hz. The step potential was 2 mV; the bottom liquid pH was 4.68.

Enrichment is the primary process during the detection of heavy metal ions by square wave stripping voltammetry. The enrichment time directly affects the intensity of the stripping peak current of the ions. Cd^{2+} and Pb^{2+} were detected simultaneously in a solution containing the two ions, and the peak current intensity of each ion for different enrichment times was recorded. Fig. 4(a) shows the stripping curves of Cd^{2+} and Pb^{2+} for different enrichment times. It can be seen from Fig. 4(a) that the enrichment time had little effect on the stripping peak current of Cd^{2+}. As the enrichment time increased, the stripping peak current value of Cd^{2+} varied from 8–11 μA. In contrast, the enrichment time had a significant effect on the peak current of Pb^{2+}. For enrichment times below 100 s, the peak current of Pb^{2+} was only 14 μA. When the enrichment time was increased to 150 s, the stripping peak current increased to 23 μA. When the enrichment time was increased further to 200 s, the peak current reached a maximum of 38 μA, while for an enrichment time of 250 s, the stripping peak current decreased to 29 μA. Fig. 4(b) shows the peak current intensity of Cd^{2+} and Pb^{2+} as a function of enrichment time. It can be seen from Fig. 4(b) that the stripping peak currents of Cd^{2+} and Pb^{2+} were affected by the enrichment time, first increasing and then decreasing as the enrichment time was increased. The effect of enrichment time on the stripping peak current of these two ions was divided into three stages. In stage **I** (50–100 s), as the enrichment time increased, the peak currents of Cd^{2+} and Pb^{2+} gradually increased but remained at a low level. This was because before 100 s, the enrichment time was too short, with few reactive ions on the electrode surface, resulting in a small stripping current value and a low growth rate for the peak current. In stage **II** (100–200 s), the peak currents of Cd^{2+} and Pb^{2+} increased, reaching a maximum at 200 s. After 100 s, Cd^{2+} and Pb^{2+} could be rapidly reduced on the electrode surface. The ion content of the surface of the electrode increased rapidly, and the growth rate of the peak current increased. At 200 s, the heavy metal ions being reduced on the surface of the electrode were almost saturated and the peak current of the dissolution reached a maximum. In stage **III** (after 200 s), the material enriched on the surface of the electrode was mainly

impurity ions from the solution. Prolonging the enrichment time led to a decrease in the intensity of the peak current. It was concluded that 200 s was the optimum enrichment time.

3.2.2 Effect of electrode surface state on stripping peak currents of Cd^{2+} and Pb^{2+}

The surface state of the electrode directly affects the reaction processes of ions on the electrode surface. The hydrogen-terminated and the oxygen-terminated are the two typical surface states of the electrode. There are many C-H bonds on the surface of the hydrogen-terminated electrode (H-BDD). Similarly, there are many C-O bonds on the surface of the oxygen-terminated electrode (O-BDD).To study the effect of the electrode surface state, we used an enrichment time of 200 s, and a mixed solution of Cd^{2+} and Pb^{2+} to simultaneously detect these ions using a BDD electrode with the two surface states. The stripping curves of Cd^{2+} and Pb^{2+} in two surface states were recorded to investigate the effect of electrode surface state on peak current.

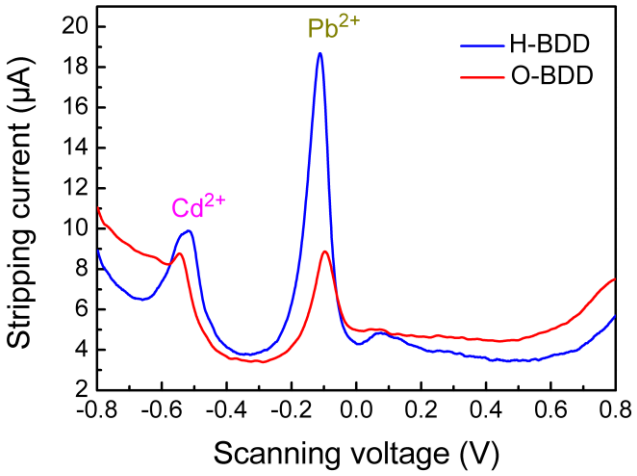

Figure 5. Stripping curves of Cd^{2+} and Pb^{2+} in two electrode surface states. The enrichment time was 200 s. The other conditions were the same as those in Fig. 4.

It can be seen from Fig. 5 that the stripping peak current values of Cd^{2+} and Pb^{2+} with the H-BDD electrode were higher, and the peak shape better defined, than with the O-BDD electrode. With the O-BDD electrode, the stripping peak current of Cd^{2+} was small, and the peak shape was defective, with the peak bottom data being lost. With the H-BDD electrode, the peak shape of Cd^{2+} was well defined, the peak bottom data was complete, and the peak current value was higher than for the O-BDD electrode. Complete stripping peaks were found for Pb^{2+} with both the O-BDD and H-BDD electrodes; however, the peak current values of Pb^{2+} were significantly different for the two surface states. The peak current value with the H-BDD electrode was 2.1 times that of the O-BDD electrode. The surface of an H-BDD electrode contains a large number of C-H groups. These C-H groups are hydrophobic and have a low electron binding energy, which contributes to an increase in the current response of Cd^{2+} and Pb^{2+} and to the electrochemical reaction rates on the electrode surface [14]. It

was concluded that the hydrogen terminated BDD electrode was more suitable for the simultaneous detection of Cd^{2+} and Pb^{2+} than the O-BDD electrode.

In summary, when the enrichment time was 200 s and the electrode surface state was hydrogen terminated, the stripping peaks of Cd^{2+} and Pb^{2+} were more complete, and the stripping peak values were at their highest, leading to a more stable detection performance of the electrode.

3.3 Calibration curve and spike recovery of BDD electrodes for simultaneous detection of Cd^{2+} and Pb^{2+}

3.3.1 Calibration curve

A linear correlation of the calibration curve reflects the detection precision of the electrode. A series of mixed standard solutions for Cd^{2+} and Pb^{2+} were prepared. BDD electrodes were used for simultaneous detection of these ions and calibration curves were drawn showing the relationship between ion concentration and peak current.

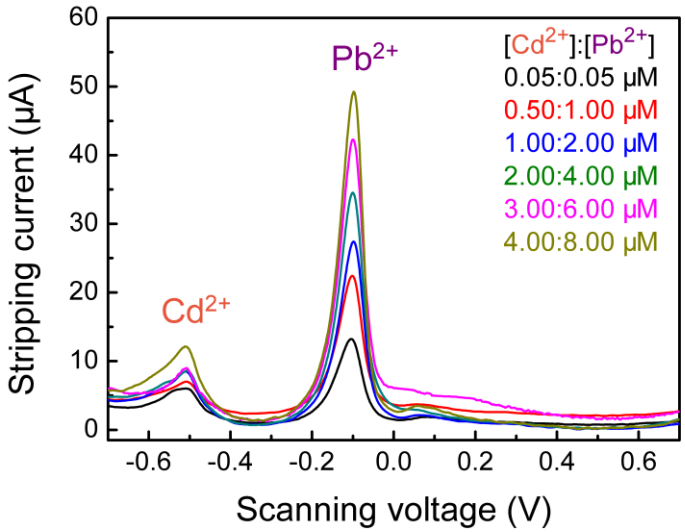

Figure 6. Stripping curves for six concentrations of standard mixed solutions. The electrode surface state was hydrogen termination. All other conditions were the same as those in Fig. 5.

It can be seen from Fig. 6 that the peak currents of Cd^{2+} and Pb^{2+} gradually increased with increasing concentration. In the concentration range of 0.05–8 μM, the peak current value of Pb^{2+} increased with an increase in the ion concentration, and the magnitude of each increase was similar. Similarly, the peak current value of Cd^{2+} increased with increasing ion concentration in the concentration range of 0.05–4 μM. However, the increase in the peak current value of Cd^{2+} was not as uniform as for Pb^{2+}. When the concentration of Cd^{2+} increased from 2 μM to 3 μM, the growth rate in the peak current dropped and may cause the linear relationship to decrease. When the concentration of Pb^{2+} increased from 0.05 μM to 8 μM, the peak current growth rate was uniform and the linear relationship was excellent. As can be seen from Fig. 7, the linear ranges of Cd^{2+} and Pb^{2+} were 0.05–4

μM and 0.05–8 μM, respectively. For Cd^{2+} and Pb^{2+} in their concentration range, there was a linear increase in the stripping current with an increase in ion concentration. The linear correlation coefficients (R^2) for Cd^{2+} and Pb^{2+} were 0.995 and 0.998, respectively. Such high linear correlations should ensure a high detection precision for the electrode [15].

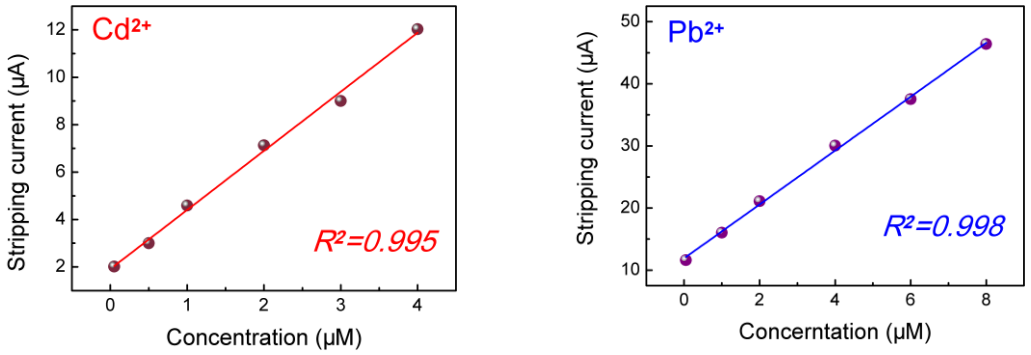

Figure 7. Calibration curves of Cd^{2+} and Pb^{2+}

The linear correlation coefficient of the calibration curve of the ion being measured reflects the detection precision of an electrode and is an important evaluation parameter for electrode detection performance. The detection performance of commonly used mercury film electrodes has been significantly improved in recent years. A typical example is that of Raquel Güell et al [16]. They integrated screen-printed mercury film electrodes in a flow system for monitoring Cd^{2+} and Pb^{2+} in water samples. The R^2 values of Cd^{2+} and Pb^{2+} they reported were 0.991 and 0.989, respectively. By comparison, the linear correlation coefficient of our BDD electrode for Cd^{2+} and Pb^{2+}, and hence the detection precision, was better than that of the mercury film electrode.

3.3.2 Spike recovery

The spiked recovery rate represents the degree of loss of the ions being tested during the detection process, and directly reflects the accuracy of the electrodes. Three different concentrations of Cd^{2+} and Pb^{2+} were added to the mixed solution and the BDD electrode used for simultaneous detection. The recoveries of the spiked samples under each spike were calculated.

Table 1. Spiked recovery of Cd^{2+} and Pb^{2+}. All conditions were the same as those in Fig. 6.

Ion species	Initial concentration	Additional concentration	Recovery rate
Cd^{2+}	0.01 mg/L	0.005 mg/L	93.5%
		0.01 mg/L	99.4%
		0.015 mg/L	95.8%
Pb^{2+}	0.05 mg/L	0.025 mg/L	93.7%
		0.05 mg/L	96.4%
		0.075 mg/L	101.3%

It can be seen in Table 1 that the spiked recoveries of Cd^{2+} and Pb^{2+} ranged from 93.5% to 99.4% and 93.7% to 101.3%, respectively. Chinese National Standard GB/T 27404-2008 gives the reference range of the recovery rate, when the content of the analyte is 0.1–1 mg/L, as between 80% and 110% [17]. The recovery rate performance of the BDD electrode for these two ions clearly meet the performance requirements of this national standard.

Luiz Fernando Ribeiro et al. have reported related work optimizing the spike recovery of mercury film electrodes [18]. They pre-coated a mercury film on the surface of screen-printed electrodes and simultaneously detected Cd^{2+} and Pb^{2+} in tap water by square wave stripping voltammetry. The results showed that the total recoveries of Cd^{2+} and Pb^{2+} were 101–118%. The overall range of recovery of the two ions from the BDD electrode was in a narrower range of 93.5–101.3%. The degree of ion loss during the detection process was significantly lower for the BDD electrode. It can be seen that our BDD electrode was more accurate than that of the mercury film electrode currently used and it is expected to meet the requirements of accuracy for in-situ detection in water sources.

3.4 Detection limit and reproducibility of BDD electrodes for simultaneous detection of Cd^{2+} and Pb^{2+}

3.4.1 Detection limit

The detection limit is the lower limit of the detection range of the electrode, which determines the application range of the electrode. In this paper, the detection limit of the electrode for these two ions was calculated as the concentration of analyte that was three times the noise of the blank response signal.

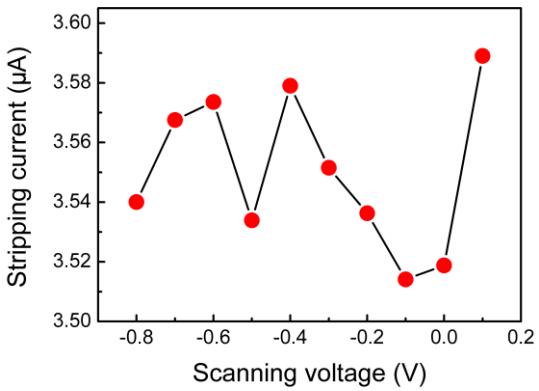

Figure 8. Scanning image of the blank control experiment of the BDD electrode. All conditions were the same as those in Fig. 6.

The blank control sample was scanned by the electrode system, the detection data was recorded every 100 mV, and ten points were used to calculate the electrode noise. Figure 8 shows the scan results of the blank control test of the BDD electrode. The stripping current obtained by scanning the

blank sample was between 3.53 μA and 3.59 μA; this range was narrow, and the current was small. The noise was calculated as the relative standard deviation of the ten scanning points and found to be 0.0259. The detection limits (D=3N/S) of Pb^{2+} and Cd^{2+} were calculated as 3.39 μg/L and 3.62 μg/L, respectively.The detection limit is an important parameter for the BDD electrode in meeting the application requirements, and it is also an important reference for improving the performance of the mercury film electrode. Chinese National Standard GB 5749-2006 stipulates that the content of Cd^{2+} and Pb^{2+} in drinking water should not exceed 0.01 mg/L and 0.05 mg/L, respectively [19]. It is clear that the detection limit of our BDD electrode is far lower than the safe concentrations of these ions in drinking water. Consequently, this electrode could be used for the detection of Cd^{2+} and Pb^{2+} ions in drinking water for water sources in rural areas. Jiri Kudr et al. developed an automatic detection system combining a mercury film electrode and an artificial neural network for the simultaneous detection of Cd^{2+} and Pb^{2+} in solution [20]. The detection limits of Cd^{2+} and Pb^{2+} obtained by them were 60 μg/L and 30 μg/L, respectively. The BDD electrode we developed reduces the detection limits of Cd^{2+} and Pb^{2+} by about 17 times and 8 times, respectively, and significantly improves on the detection limit of the mercury membrane electrode.

3.4.2 Reproducibility

Reproducibility reflects the degree of attenuation in the electrode detection performance as the number of detections increases. The reproducibility of multiple repetitive experiments can reflect the precision of the electrodes. The mixed solution was subjected to seven repeatability tests using a BDD electrode, and the relative standard deviation of the measurements was calculated. As can be seen from Fig. 9, the stripping curves of the seven repetitive experiments largely coincided, indicating that detection of both Cd^{2+} and Pb^{2+} had good reproducibility.

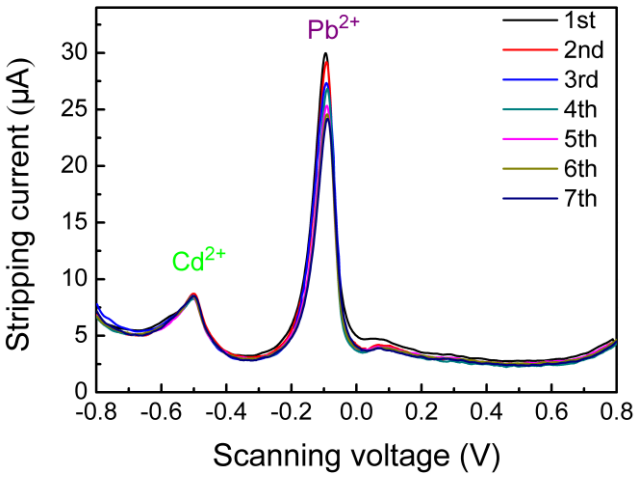

Figure 9. Stripping curves of seven repetitive experiments. All conditions were the same as those in Fig. 6.

The stripping peak potential of these two ions did not change significantly with an increase in the number of detections. The peak shape of each ion and the peak bottom data were complete. The peak current values of Cd^{2+} and Pb^{2+} decreased slightly, but still remained at acceptable levels. For Cd^{2+} especially, the peak current value was essentially unchanged, demonstrating excellent reproducibility. After seven repetitive tests, the relative standard deviations of Cd^{2+} and Pb^{2+} were calculated to be 1.103% and 3.819%, respectively.

The reproducibility and precision of the electrode are important criteria for assessing the detection performance of an electrode and are useful parameters in comparing the performance of the mercury film electrode with our BDD electrode. Many researchers are working to improve the reproducibility of mercury film electrodes to expand their application in water quality testing. A typical example is the work of Silvia Illuminati et al [21]. They used a mercury film electrode prepared by electrochemical deposition to simultaneously detect Cd^{2+} and Pb^{2+} in solution. For Cd^{2+} and Pb^{2+} in reproducibility experiments, the lowest relative standard deviations of the mercury film electrodes, after optimizing the operating parameters, were 6% and 5%, respectively. It is clear that our BDD electrode has much better reproducibility and a higher precision than the mercury film electrode, effectively overcoming the disadvantages of the performance degradation of the mercury film electrode.

3.5 Comparison of detection performance of similar BDD electrodes

To measure the detection performance of our BDD electrode, we compared it with similar BDD electrodes reported in the literature.

It can be seen from Table 2 that of the four detection systems, the BDD electrode we developed had both excellent linear range and spiked recovery range, with a level of reproducibility similar to the other electrodes, but a slightly higher detection limit. Our BDD electrode has a very wide linear range and a narrower spike recovery range than the other electrodes, which would allow for greater precision if used for in-situ monitoring of water quality. The reproducibility of our electrode was similar to that of other BDD electrodes, which would ensure the precision and performance stability required by in-situ monitoring systems used in water sources in rural areas. Although the detection limit for our electrode was slightly higher than that of some similar electrodes, it was still well within the concentration range specified by the Chinese national standards.

Table 2. Comparison of detection performance of our BDD electrode with those reported in the literature, where DPASV indicates differential pulse anodic stripping voltammetry and SWASV indicates square wave anodic stripping voltammetry

Mode	Linear range (μg/L)	Spike recovery range	Detection limit (μg/L)	RSD	Ref.
SWASV	Cd^{2+}:1-20	--	Cd^{2+}:0.894	--	22
DPASV	Pb^{2+}:129-918	--	Pb^{2+}:0.4	--	23
DPASV	Cd^{2+}:5-100	--	Cd^{2+}:3.5	Cd^{2+}:5.0%	24

	Pb^{2+}:5-100		Pb^{2+}:2.0	Pb^{2+}:4.8%	
DPASV	--	--	Cd^{2+}:2.47 Pb^{2+}:51.5	Cd^{2+}:3.0% Pb^{2+}:2.0%	25
SWASV	--	93.3%-109%	Cd^{2+}:0.18 Pb^{2+}:0.08	--	26
SWASV	Cd^{2+}:5.6-448 Pb^{2+}:10.3-1648	93.5%-101.3%	Cd^{2+}:3.39 Pb^{2+}:3.62	Cd^{2+}:1.103% Pb^{2+}:3.819%	This work

4. CONCLUSIONS

In-situ monitoring of heavy metal ions in water sources in rural areas is the only way to prevent pollution of these water sources. Unfortunately, the existing mercury film electrodes have the disadvantage of secondary pollution and performance degradation. In this study, BDD electrodes were prepared and the process parameters optimized. The detection performance of the electrodes was systematically investigated, through characterization of the microstructure and electrochemical properties of the electrode and its operating parameters. The electrode was used to simultaneously detect Cd^{2+} and Pb^{2+} in mixed solutions of these ions and calibration curves, spike recovery, detection limit and reproducibility were determined. The main conclusions were:

(1) Optimizing the operating parameters of the BDD electrode significantly improved the detection precision of the electrode. The optimum working parameters were an enrichment time of 200 s and a hydrogen-terminated electrode surface. The shapes of stripping peaks of Cd^{2+} and Pb^{2+} thus obtained were complete, and the peak values were at a maximum. These parameters meet the high detection precision requirements for the electrode.

(2) The BDD electrode had excellent detection precision and accuracy, allowing the simultaneous detection of Cd^{2+} and Pb^{2+} under conditions which do not affect the environment. There was a very good linear relationship between the concentration and the stripping peak current, for both Cd^{2+} and Pb^{2+}. The linear ranges were 0.05–4 μM and 0.05–8 μM, and the R^2 values for the calibration curves were 0.995 and 0.998, respectively. The spiked recovery range was narrow with an overall range of 93.5–101.3%, and the accuracy of the electrode was high.

(3) The low detection limit and high reproducibility of the BDD electrodes, together with a wide application range and high precision, mean that they can effectively overcome the shortcomings of secondary pollution and performance degradation found with mercury film electrodes. The detection limits were low for both Cd^{2+} and Pb^{2+} and were determined as 3.39 μg/L and 3.62 μg/L, respectively. The reproducibility was good, with RSDs, obtained from seven repeated experiments, for Cd^{2+} and Pb^{2+} of 1.103% and 3.819%, respectively.

The BDD electrode developed in this work effectively overcomes the shortcomings of secondary pollution and performance degradation encountered with mercury film electrodes and can meet the long duration application requirements needed for simultaneous detection by in-situ monitoring systems. The BDD electrode could be used for in-situ detection and early warning of heavy metal ions in water sources in rural areas.

ACKNOWLEDGEMENTS
This work is supported by the National Natural Science Foundation of China (Grant No. 51571183) and the Fundamental Research Funds for the Central Universities of China.

References

1. X.Y. Bi, Z.G. Li, S.X. Wang, L. Zhang, R. Xu, J.L. Liu, H.M. Yang and M.Z. Guo, *Environ. Sci. Technol.*, 51 (2017) 13502.
2. A. Shah, S. Sultan, A. Zahid, S. Aftab, J. Nisar, S. Nayab, R. Qureshi, G.S. Khan, H. Hussain and S.A. Ozkan, *Electrochim Acta*, 258 (2017) 1397.
3. B. Petovar, K. Xhanari and M. Finšgar, *Anal. Chim. Acta*, 1004 (2018) 10.
4. A. Economou, *Sensors*, 18 (2018) 1032.
5. S.G.R. Avuthu, J.T. Wabeke, B.B. Narakathu, D. Maddipatla, J.S. Arachchilage, S.O. Obare and M.Z. Atashbar, *IEEE. Sens. J.*, 16 (2016) 8678.
6. F.W.P. Ribeiro, C.P. Sousa, S. Morais, P. de Lima-Neto and A.N. Correia, *Microchem. J.*, 142 (2018) 24.
7. Y.P. He, W.M. Huang, R.L. Chen, W.L. Zhang, H.B. Lin and H.D. Li, *Sep. Purif. Technol*., 156 (2015) 124.
8. S. Pysarevska, L. Dubenska, S. Plotycya and L. Svorc, *Sens. Actuators, B*, 270 (2018) 9.
9. S. Djurdjic, V. Vukojevic, S. Jevtic, M.V. Pergal, B.B. Petkovic and D.M. Stankovic, *Int. J. Electrochem. Sci*., 13 (2018) 2791.
10. A. Pop, S. Lung, C. Orha and F. Manea, *Int. J. Electrochem. Sci*., 13 (2018) 2651.
11. Y. Li, H. Li, M. Li, C. Li, D. Sun and B. Yang, *Electrochim Acta*, 258 (2017) 744.
12. S. Nantaphol, T. Watanabe and N. Nomura, *Biosens. Bioelectron*., 98 (2017) 76.
13. E. Mehmeti, D.M. Stankovic, A. Ortner, J. Zavasnik and K. Kalcher, *Food. Anal. Method.*, 10 (2017) 3747.
14. S. Kasahara, K. Natsui, T. Watanabe, Y. Yokota, Y. Kim, S. Iizuka, Y. Tateyama and Y. Einaga, *Anal. Chem*., 89 (2017) 11341.
15. D.K. Belghiti, E. Scorsone, J. De Sanoit and P. Bergonzo, *Phys. Status Solidi A*, 213 (2016) 10.
16. R. Güell, C. Fontàs, G. Aragay, A. Merkoçi and E. Anticó, *Int. J. Environ. An. Ch*., 93 (2013) 12.
17. C. Ding, W. Cheng, X. Wang, Z.Y. Wu, Y. Sun, C. Chen, X.K. Wang and S.H. Yu, *J. Hazard. Mater*., 313 (2016) 253.
18. L.F. Ribeiro and J.C. Masini, *Electroanalysis*, 26 (2014) 2745.
19. B. Qu, Y. Zhang, S. Kang and M. Sillanpää, *Sci. Total. Environ*., 649 (2018) 571.
20. J. Kudr, H.V. Nguyen, J. Gumulec, L. Nejdl, I. Blazkova, B. Ruttkay-Nedecky, D. Hynek, J. Kynicky, V. Adam and R. Kizek, *Sensors*, 15 (2015) 592.
21. S. Illuminati, A. Annibaldi, C. Truzzi, C. Finale and G. Scarponi, *Electrochim Acta*, 104 (2013) 148.
22. S. André F, T.M. Arantes, F.H. Cristovan and N.G. Ferreira, *Thin Solid Films*, 625 (2017) 70.
23. G.G. Honorio, G.C. Azevedo, M.A.C. Matos, M.A.L. de Oliveira and R.C. Matos, *Food Control*, 36 (2014) 42.
24. J.H. Yoon, J. Yang, J. Kim, J. Bae, Y.B. Shim and M.S. Won, *B. Korean. Chem. Soc*., 31 (2010) 140.
25. A. Zazoua, N. Khedimallah and N. Jaffrezic-Renault, *Anal. Lett*., 51 (2018) 336.
26. V.B.D. Santos, E.L. Fava, N.S.D.M. Curi, R.C. Faria, T.B. Guerreiro and O. Fatibellofilho, *Analytical Methods*, 7 (2015) 3105.